

# Activation measurement of the ${}^3\text{He}(\alpha, \gamma){}^7\text{Be}$ cross section at low energy

D. Bemmerer,<sup>1</sup> F. Confortola,<sup>2</sup> H. Costantini,<sup>2</sup> A. Formicola,<sup>3</sup> Gy. Gyürky,<sup>4</sup> R. Bonetti,<sup>5</sup> C. Broggini,<sup>1,\*</sup> P. Corvisiero,<sup>2</sup> Z. Elekes,<sup>4</sup> Zs. Fülöp,<sup>4</sup> G. Gervino,<sup>6</sup> A. Guglielmetti,<sup>5</sup> C. Gustavino,<sup>3</sup> G. Imbriani,<sup>7</sup> M. Junker,<sup>3</sup> M. Laubenstein,<sup>3</sup> A. Lemut,<sup>2</sup> B. Limata,<sup>7</sup> V. Lozza,<sup>1</sup> M. Marta,<sup>5</sup> R. Menegazzo,<sup>1</sup> P. Prati,<sup>2</sup> V. Roca,<sup>7</sup> C. Rolfs,<sup>8</sup> C. Rossi Alvarez,<sup>1</sup> E. Somorjai,<sup>4</sup> O. Straniero,<sup>9</sup> F. Strieder,<sup>8</sup> F. Terrasi,<sup>10</sup> and H.P. Trautvetter<sup>8</sup>

(The LUNA Collaboration)

<sup>1</sup>*Istituto Nazionale di Fisica Nucleare (INFN), Sezione di Padova, via Marzolo 8, 35131 Padova, Italy*

<sup>2</sup>*Università di Genova and INFN Sezione di Genova, Genova, Italy*

<sup>3</sup>*INFN, Laboratori Nazionali del Gran Sasso (LNGS), Assergi (AQ), Italy*

<sup>4</sup>*Institute of Nuclear Research (ATOMKI), Debrecen, Hungary*

<sup>5</sup>*Istituto di Fisica Generale Applicata, Università di Milano and INFN Sezione di Milano, Italy*

<sup>6</sup>*Dipartimento di Fisica Sperimentale, Università di Torino and INFN Sezione di Torino, Torino, Italy*

<sup>7</sup>*Dipartimento di Scienze Fisiche, Università di Napoli "Federico II", and INFN Sezione di Napoli, Napoli, Italy*

<sup>8</sup>*Institut für Experimentalphysik III, Ruhr-Universität Bochum, Bochum, Germany*

<sup>9</sup>*Osservatorio Astronomico di Collurania, Teramo, and INFN Sezione di Napoli, Napoli, Italy*

<sup>10</sup>*Seconda Università di Napoli, Caserta, and INFN Sezione di Napoli, Napoli, Italy*

(Dated: July 5, 2006)

The nuclear physics input from the  ${}^3\text{He}(\alpha, \gamma){}^7\text{Be}$  cross section is a major uncertainty in the fluxes of  ${}^7\text{Be}$  and  ${}^8\text{B}$  neutrinos from the Sun predicted by solar models and in the  ${}^7\text{Li}$  abundance obtained in big-bang nucleosynthesis calculations. The present work reports on a new precision experiment using the activation technique at energies directly relevant to big-bang nucleosynthesis. Previously such low energies had been reached experimentally only by the prompt- $\gamma$  technique and with inferior precision. Using a windowless gas target, high beam intensity and low background  $\gamma$ -counting facilities, the  ${}^3\text{He}(\alpha, \gamma){}^7\text{Be}$  cross section has been determined at 127, 148 and 169 keV center-of-mass energy with a total uncertainty of 4%. The sources of systematic uncertainty are discussed in detail. The present data can be used in big-bang nucleosynthesis calculations and to constrain the extrapolation of the  ${}^3\text{He}(\alpha, \gamma){}^7\text{Be}$  astrophysical S-factor to solar energies.

PACS numbers: 25.55.-e, 26.20.+f, 26.35.+c, 26.65.+t

The  ${}^3\text{He}(\alpha, \gamma){}^7\text{Be}$  reaction is a critical link in the  ${}^7\text{Be}$  and  ${}^8\text{B}$  branches of the proton-proton (p-p) chain of solar hydrogen burning [1]. At low energies its cross section  $\sigma(E)$  ( $E$  denotes the center of mass energy,  $E_\alpha$  the  ${}^4\text{He}$  beam energy in the laboratory system) can be parameterized by the astrophysical S-factor  $S(E)$  defined as

$$S(E) = \sigma(E) \cdot E \exp(2\pi\eta(E))$$

with  $\eta(E) \propto E^{-0.5}$  [2]. The 9.4% uncertainty [3] in the S-factor extrapolation to the solar Gamow energy (23 keV) contributes 8% to the uncertainty in the predicted fluxes of solar neutrinos from the decays of  ${}^7\text{Be}$  and  ${}^8\text{B}$  [4]. The interior of the Sun, in turn, can be studied [4, 5] by comparing this prediction with the data from neutrino detectors [6, 7], which determine the  ${}^8\text{B}$  neutrino flux with a total uncertainty as low as 3.5% [7].

Furthermore, the production of  ${}^7\text{Li}$  in big-bang nucleosynthesis (BBN) is highly sensitive to the  ${}^3\text{He}(\alpha, \gamma){}^7\text{Be}$  cross section in the energy range  $E \approx 160\text{--}380$  keV [8], with an adopted uncertainty of 8% [9]. Based on the baryon-to-photon ratio from observed anisotropies in the cosmic microwave background [10], network calculations predict primordial  ${}^7\text{Li}$  abundances [11] that are significantly higher than observations [12, 13]. A lower  ${}^3\text{He}(\alpha, \gamma){}^7\text{Be}$  cross section at relevant energies may explain part of this discrepancy.

The  ${}^3\text{He}(\alpha, \gamma){}^7\text{Be}$  ( $Q$ -value: 1.586 MeV) reaction leads to the emission of prompt  $\gamma$ -rays, and the final  ${}^7\text{Be}$  nucleus decays with a half-life of  $53.22 \pm 0.06$  days, emitting a 478 keV  $\gamma$ -ray in  $10.44 \pm 0.04\%$  of the cases [14]. The cross section can be measured by detecting either the induced  ${}^7\text{Be}$  activity (activation method) or the prompt  $\gamma$ -rays from the reaction (prompt- $\gamma$  method). Previous activation studies [15, 16, 17, 18] cover the energy range  $E = 420\text{--}2000$  keV. Prompt  $\gamma$ -ray measurements [15, 19, 20, 21, 22, 23, 24] cover  $E = 107\text{--}2500$  keV, although with limited precision at low energies.

The global shape of the S-factor curve is well reproduced by theoretical calculations [25, 26]. However, the slope has been questioned [26] for  $E \leq 300$  keV, where there are no high-precision data. Furthermore, a global analysis [3] indicates that S-factor data obtained with the activation method are systematically higher than the prompt- $\gamma$  results. A recent activation study [18] reduces this discrepancy to 9% for the extrapolated  $S(0)$  [3], still not at the precision level of the  ${}^8\text{B}$  neutrino data [7]. Precise  ${}^3\text{He}(\alpha, \gamma){}^7\text{Be}$  measurements at low energies have been recommended to study the solar interior [4, 5, 27], to sharpen big-bang  ${}^7\text{Li}$  abundance predictions [8, 28], and to investigate the low-energy slope of the S-factor curve [26]. The aim of the present work is to provide high precision activation data at energies directly relevant to

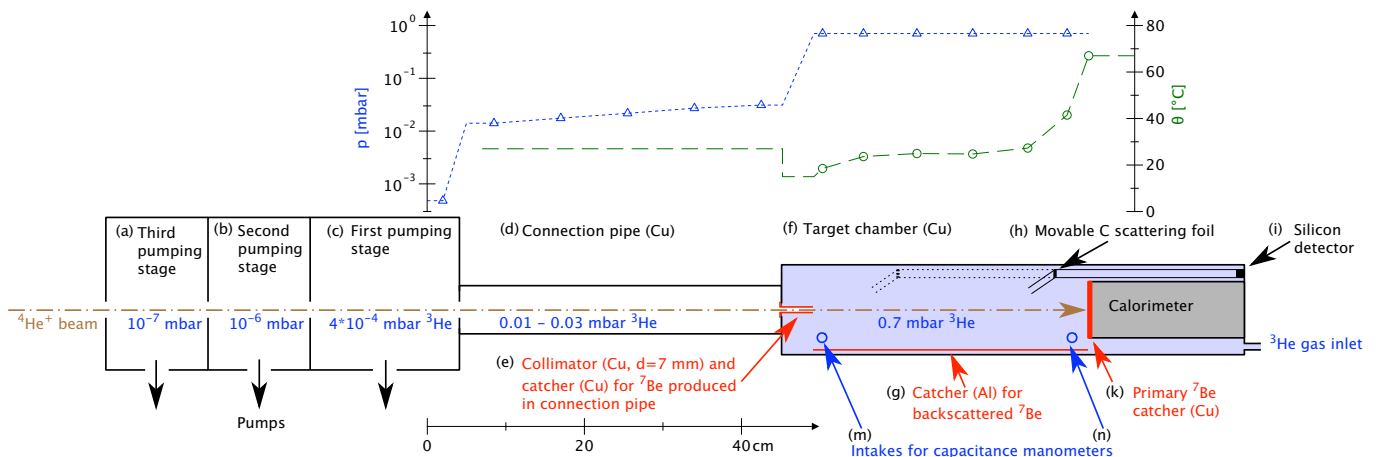


FIG. 1: Schematic view of the target chamber used for the irradiations. Above: pressure ( $p$ , triangles) and temperature ( $\theta$ , circles) values measured without ion beam and interpolated profile between the data points (lines). See text for details.

big-bang nucleosynthesis and low enough to effectively constrain the extrapolation to solar energies.

The Laboratory for Underground Nuclear Astrophysics (LUNA) [29] in Italy's Gran Sasso underground laboratory (LNGS) has been designed for measuring low nuclear cross sections for astrophysical purposes [30, 31, 32, 33, 34, 35]. The irradiations have been carried out at the 400 kV LUNA2 accelerator [36] at energies  $E_\alpha = 300, 350$  and  $400$  keV, with a typical current of  $200 \mu\text{A}$   $^4\text{He}^+$ . The beam energy is obtained from a precision resistor chain and has  $5 \text{ eV/h}$  long-term stability [36]. The  $^3\text{He}(\alpha, \gamma)^7\text{Be}$  reaction takes place in a differentially pumped windowless gas target (Fig. 1, similar to the one described previously [37]) filled with enriched  $^3\text{He}$  gas (isotopic purity  $>99.95\%$ , pressure  $0.7$  mbar, target thickness  $9\text{--}10$  keV). The exhaust from the first and second pumping stages is cleaned in a getter-based gas purifier and recirculated into the target. The ion beam from the accelerator passes three pumping stages (Fig. 1 a-c), a connection pipe (d), enters the target chamber (f) through an aperture of  $7$  mm diameter (e) and is finally stopped on a detachable oxygen free high conductivity (OFHC) copper disk (k) of  $70$  mm diameter that serves as the primary catcher for the produced  $^7\text{Be}$  and as the hot side of a calorimeter with constant temperature gradient [37]. A precision of  $1.5\%$  for the beam intensity is obtained from the difference between the calorimeter power values with and without incident ion beam, taking into account the calculated energy loss in the target gas [38] and using a calibration curve determined by measuring the electrical charge in the same setup without gas, applying a proper secondary electron suppression voltage. The effective target thickness depends on the pressure (monitored during the irradiations with two capacitance manometers, Fig. 1 m-n), the pressure and temperature profile (measured without ion beam, resulting density uncertainty  $0.6\%$ ), the thinning of the target

gas through the beam heating effect [39] and the fraction of gases other than  $^3\text{He}$ . In order to study the latter two effects, a  $100 \mu\text{m}$  thick silicon detector (Fig. 1 i) detects projectiles that have been elastically scattered first in the target gas and subsequently in a movable  $15 \mu\text{g}/\text{cm}^2$  carbon foil (h). The beam heating effect has been investigated in a wide beam energy and intensity range, and a correction of  $4.9 \pm 1.3\%$ ,  $5.4 \pm 1.3\%$  and  $5.7 \pm 1.3\%$  was found for the irradiations at  $E_\alpha = 300, 350$  and  $400$  keV, respectively. The amount of contaminant gases (mainly nitrogen) is monitored with the silicon detector during the irradiations, kept below  $1.0 \pm 0.1\%$  and corrected for in the analysis. Further details of the elastic scattering measurements are described elsewhere [40].

The catchers are irradiated with charges of  $60\text{--}220$  C, accumulating  $^7\text{Be}$  activities of  $0.2\text{--}0.5$  Bq. The effective center of mass energy  $E^{\text{eff}}$  is calculated assuming a constant S-factor over the target length [2]. The uncertainties of  $0.3$  keV in  $E_\alpha$  [36] and of  $4.4\%$  in the energy loss [38] result in an S-factor uncertainty of  $0.5\text{--}0.8\%$ . Calculations for the straggling of the  $^4\text{He}$  beam and of the produced  $^7\text{Be}$  nuclei in the  $^3\text{He}$  gas and for the emission cone of  $^7\text{Be}$  (opening angle  $1.8\text{--}2.1^\circ$ ) show that  $99.8\%$  of the  $^7\text{Be}$  produced inside the target chamber, including the  $7$  mm collimator, reaches the primary catcher.

After the irradiation, the catcher is dismantled and counted in close geometry subsequently with two  $120\%$  relative efficiency HPGe detectors called LNGS1 (Fig. 2) and LNGS2, both properly shielded with copper and lead, in the LNGS underground counting facility [41]. Detector LNGS1 is additionally equipped with an anti-radon box, and its laboratory background is two orders of magnitude lower than with equivalent shielding overground [41]. In order to obtain the photopeak counting efficiencies, three homogeneous  $^7\text{Be}$  sources of  $200\text{--}800$  Bq activity and  $8$  mm active diameter were prepared with the  $^7\text{Li}(p,n)^7\text{Be}$  reaction at ATOMKI. Their activity

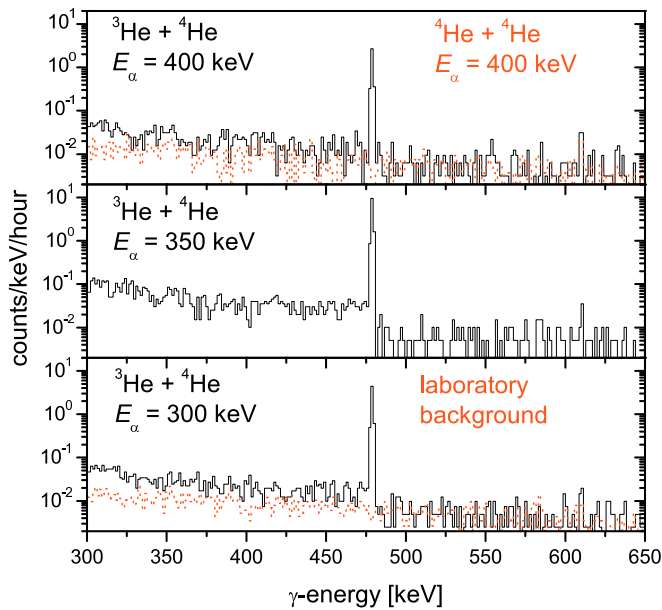


FIG. 2: Offline  $\gamma$ -counting spectra, detector LNGS1. Solid black line:  $^3\text{He}$  gas bombarded at  $E_\alpha = 400, 350, 300$  keV (top to down), respectively. Dotted red line, top panel:  $^4\text{He}$  gas bombarded at  $E_\alpha = 400$  keV. Dotted red line, bottom panel: laboratory background.

TABLE I: Systematic uncertainties in the  $^3\text{He}(\alpha, \gamma)^7\text{Be}$  astrophysical S-factor, neglecting contributions below 0.2%.

Source	Uncertainty
$^7\text{Be}$ counting efficiency	1.8 %
Beam intensity	1.5 %
Beam heating effect	1.3 %
Target pressure and temperature without beam	0.6 %
$^7\text{Be}$ backscattering	0.5 %
Incomplete $^7\text{Be}$ collection	0.4 %
$^7\text{Be}$ distribution in catcher	0.4 %
478 keV $\gamma$ -ray branching [14]	0.4 %
Effective energy	0.5–0.8 %
Total:	2.9–3.0 %

was determined with two HPGe detectors (each efficiency based on an independent set of commercial  $\gamma$ -ray sources) at ATOMKI and with one HPGe detector, called LNGS3 (efficiency based on a third set of commercial sources), at LNGS, giving consistent results and a final activity uncertainty of 1.8%. The three  $^7\text{Be}$  sources were then used to calibrate detectors LNGS1 and LNGS2 in the same geometry as the activated samples. The  $^7\text{Be}$  distribution in the catchers has been calculated from the  $^7\text{Be}$  emission angle and straggling, and GEANT4 [42] simulations gave  $0.8 \pm 0.4\%$  to  $1.0 \pm 0.4\%$  correction for the  $\gamma$ -ray efficiency because of the tail of the distribution at high radii.

In order to investigate parasitic production of  $^7\text{Be}$

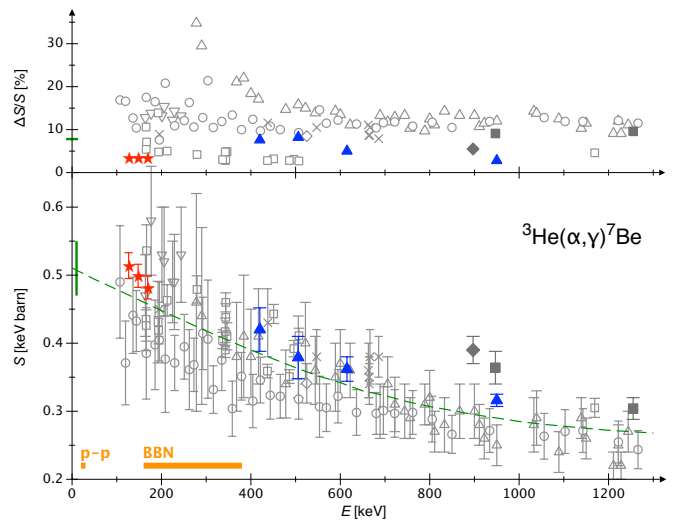


FIG. 3: Lower panel: astrophysical S-factor for  $^3\text{He}(\alpha, \gamma)^7\text{Be}$ . Activation data: filled squares [15], filled diamonds [16], filled triangles [18], stars (present work). Prompt- $\gamma$  data: triangles [20], inverted triangles [21], circles [22] (renormalized by a factor 1.4 [24]), squares [15], diamonds [23], crosses [24]. Dashed line: previously adopted R-matrix fit [9]. Horizontal bars: energies relevant for p-p chain and for BBN. — Upper panel: uncertainties (systematic and statistical combined in quadrature) of the data and of the R-matrix  $S(0)$  [9].

through, e.g., the  $^6\text{Li}(d, n)^7\text{Be}$  and  $^{10}\text{B}(p, \alpha)^7\text{Be}$  reactions induced by possible traces of  $^2\text{DH}_2^+$  in the  $^4\text{He}^+$  beam, the enriched  $^3\text{He}$  target gas was replaced with 0.7 mbar  $^4\text{He}$ , and a catcher was bombarded at the highest available energy of  $E_\alpha = 400$  keV. Despite the high applied dose of 104 C, in 16 days counting time no  $^7\text{Be}$  has been detected (Fig. 2, top panel), establishing a  $2\sigma$  upper limit of 0.1% for parasitic  $^7\text{Be}$ .

Furthermore,  $^7\text{Be}$  losses by backscattering from the primary catcher and by incomplete collection were studied experimentally at  $E_\alpha = 400$  keV and with Monte Carlo simulations at 300, 350 and 400 keV. For the backscattering study, parts of the inner surface of the chamber were covered by aluminum foil functioning as secondary catcher (Fig. 1g). It was found that  $1.3 \pm 0.5\%$  of the created  $^7\text{Be}$  is lost due to backscattering, consistent with 1.5% obtained in a GEANT4 [42] simulation using a SRIM-like multiple scattering process [43]. At lower energies, the simulation result was used as backscattering correction (up to 2.2%, adopted uncertainty 0.5%).

Incomplete  $^7\text{Be}$  collection occurs since 3.5% of the total  $^3\text{He}$  target thickness are in the connecting pipe, and a part of the  $^7\text{Be}$  is created there does not reach the primary catcher but is instead implanted into the 7 mm collimator (Fig. 1e). At  $E_\alpha = 400$  keV, a modified collimator functioning as secondary catcher was used, and a  $2.6 \pm 0.4\%$  effect was observed, consistent with a simulation ( $2.1 \pm 0.4\%$ ). For  $E_\alpha = 300$  and 350 keV, incomplete

TABLE II: Cross section and S-factor results, relative uncertainties, and electron screening [44] enhancement factors  $f$ .

$E^{\text{eff}}$ [keV]	$\sigma(E^{\text{eff}})$ [ $10^{-9}$ barn]	$S(E^{\text{eff}})$ [keV barn]	$\Delta S/S$		$f$
			stat.	syst.	
126.5	1.87	0.514	2.0 %	3.0 %	1.012
147.7	4.61	0.499	1.7 %	2.9 %	1.009
168.9	9.35	0.482	2.0 %	2.9 %	1.008

${}^7\text{Be}$  collection was corrected for based on the simulation (up to 2.3 % correction, adopted uncertainty 0.4 %).

Sputtering losses of  ${}^7\text{Be}$  by the  ${}^4\text{He}$  beam were simulated [38], showing that for the present beam energies sputtering is  $10^4$  times less likely than transporting the  ${}^7\text{Be}$  even deeper into the catcher, so it has been neglected.

The systematic uncertainties are summarized in Table I, giving a total value of 3 %. For the present low energies an electron screening enhancement factor  $f$  [44] of up to 1.012 has been calculated in the adiabatic limit, but not corrected for (Table II).

The present data (Table II, lower panel of Fig. 3) are the first activation results at energies directly relevant to big-bang  ${}^7\text{Li}$  production. Their uncertainty of 4 % (systematic and statistical combined in quadrature) is comparable to or lower than previous activation studies at high energy and lower than prompt- $\gamma$  studies at comparable energy (upper panel of Fig. 3).

To give an estimate for the low-energy implications, rescaling the most recent R-matrix fit [9] to the present data results in  $S(0) = 0.547 \pm 0.017$  keV barn, consistent with, but more precise than, Ref. [18]. All activation data combined (Refs. [15, 16, 17, 18] and the present work) give  $S(0) = 0.550 \pm 0.012$  keV barn, higher than the weighted average of all previous prompt- $\gamma$  studies,  $S(0) = 0.507 \pm 0.016$  keV barn [3]. Prompt- $\gamma$  experiments with precision comparable to the 4 % reached in the present activation work are now called for in order to verify the normalization of the prompt- $\gamma$  data.

This work was supported by INFN and in part by: TARI RII-CT-2004-506222, OTKA T42733 and T49245, and BMBF (05CL1PC1-1).

- [1] J. N. Bahcall et al., *Astrophys. J.* **621**, L85 (2005).
- [2] C. Rolfs and W. Rodney, *Cauldrons in the Cosmos* (University of Chicago Press, Chicago, 1988).
- [3] E. Adelberger et al., *Rev. Mod. Phys.* **70**, 1265 (1998).
- [4] J. N. Bahcall and M. H. Pinsonneault, *Phys. Rev. Lett.* **92**, 121301 (2004).
- [5] G. Fiorentini and B. Ricci, astro-ph/0310753.
- [6] S. Ahmed et al., *Phys. Rev. Lett.* **92**, 181301 (2004).
- [7] J. Hosaka et al., *Phys. Rev. D* **73**, 112001 (2006).
- [8] S. Burles et al., *Phys. Rev. Lett.* **82**, 4176 (1999).
- [9] P. Descouvemont et al., *At. Data Nucl. Data Tables* **88**, 203 (2004).
- [10] D. Spergel et al., *Astrophys. J. Suppl.* **148**, 175 (2003).
- [11] A. Coc et al., *Astrophys. J.* **600**, 544 (2004).
- [12] S. Ryan et al., *Astrophys. J. Lett.* **530**, L57 (2000).
- [13] P. Bonifacio et al., *Astron. Astrophys.* **390**, 91 (2002).
- [14] D. Tilley et al., *Nucl. Phys. A* **708**, 3 (2002).
- [15] J. Osborne et al., *Phys. Rev. Lett.* **48**, 1664 (1982), *Nucl. Phys. A* **419**, 115 (1984).
- [16] R. Robertson et al., *Phys. Rev. C* **27**, 11 (1983).
- [17] H. Volk et al., *Z. Phys. A* **310**, 91 (1983).
- [18] B. N. Singh et al., *Phys. Rev. Lett.* **93**, 262503 (2004).
- [19] H. Holmgren and R. Johnston, *Phys. Rev.* **113**, 1556 (1959).
- [20] P. Parker and R. Kavanagh, *Phys. Rev.* **131**, 2578 (1963).
- [21] K. Nagatani et al., *Nucl. Phys. A* **128**, 325 (1969).
- [22] H. Kr awinkel et al., *Z. Phys. A* **304**, 307 (1982).
- [23] T. Alexander et al., *Nucl. Phys. A* **427**, 526 (1984).
- [24] M. Hilgemeier et al., *Z. Phys. A* **329**, 243 (1988).
- [25] T. Kajino, *Nucl. Phys. A* **460**, 559 (1986).
- [26] A. Cs ot o and K. Langanke, *Few-Body Systems* **29**, 121 (2000).
- [27] J. N. Bahcall et al., astro-ph/0511337.
- [28] P. Serpico et al., *J. Cosmol. Astropart. Ph.* **12**, 010 (2004).
- [29] U. Greife et al., *Nucl. Inst. Meth. A* **350**, 327 (1994).
- [30] R. Bonetti et al., *Phys. Rev. Lett.* **82**, 5205 (1999).
- [31] C. Casella et al., *Nucl. Phys. A* **706**, 203 (2002).
- [32] A. Formicola et al., *Phys. Lett. B* **591**, 61 (2004).
- [33] D. Bemmerer et al., *Eur. Phys. J. A* **24**, 313 (2005).
- [34] G. Imbriani et al., *Eur. Phys. J. A* **25**, 455 (2005).
- [35] A. Lemut et al., *Phys. Lett. B* **634**, 483 (2006).
- [36] A. Formicola et al., *Nucl. Inst. Meth. A* **507**, 609 (2003).
- [37] C. Casella et al., *Nucl. Inst. Meth. A* **489**, 160 (2002).
- [38] J. Ziegler, SRIM 2003.26, <http://www.srim.org>.
- [39] J. G orres et al., *Nucl. Inst. Meth.* **177**, 295 (1980).
- [40] M. Marta, Master's thesis, Politecnico di Milano (2005), and to be submitted to *Nucl. Inst. Meth. A*.
- [41] C. Arpesella, *Appl. Radiat. Isot.* **47**, 991 (1996).
- [42] S. Agostinelli et al., *Nucl. Inst. Meth. A* **506**, 250 (2003).
- [43] M. H. Mendenhall and R. A. Weller, *Nucl. Inst. Meth. B* **227**, 420 (2005).
- [44] H. Assenbaum et al., *Z. Phys. A* **327**, 461 (1987).

\* Corresponding author, brogini@pd.infn.it.